Stratigraphy and sedimentology of the Santa Fe Group adjoining the Little San Pascual Mountains – implications for footwall exhumation and evolution of the Little San Pascual Mountain fault zone

Daniel J. Koning and Matthew T. Heizler
2022, pp. 203-220. https://doi.org/10.56577/FFC-72.203
Supplemental data: https://nmgs.nmt.edu/repository/index.cfml?rid=2022001

in:

Socorro Region III, Koning, Daniel J.; Hobbs, Kevin J.; Phillips, Fred M.; Nelson, W. John; Cather, Steven M.; Jakle, Anne C.; Van Der Werff, Brittney, New Mexico Geological Society 72nd Annual Fall Field Conference Guidebook, 426 p. https://doi.org/10.56577/FFC-72

This page is intentionally left blank to maintain order of facing pages.

New Mexico Geological Society Guidebook, 72nd Fall Field Conference, 2022, p. 203–220.

STRATIGRAPHY AND SEDIMENTOLOGY OF THE SANTA FE GROUP ADJOINING THE LITTLE SAN PASCUAL MOUNTAINS – IMPLICATIONS FOR FOOTWALL EXHUMATION AND EVOLUTION OF THE LITTLE SAN PASCUAL MOUNTAIN FAULT ZONE

DANIEL J. KONING[1] AND MATTHEW T. HEIZLER[1]

[1]New Mexico Bureau of Geology and Mineral Resources, New Mexico Institute of Mining and Technology, 801 Leroy Place, Socorro, NM 87801; dan.koning@nmt.edu

Abstract—Detailed stratigraphic and sedimentologic investigation of the Santa Fe Group adjoining the Little San Pascual Mountains (LSPM) allows reconstruction of an exhumational history for these mountains during the middle Miocene–Quaternary. One can also interpret the evolution of the two main strands of the 035°-striking Little San Pascual Mountain fault zone (LSPMFZ) that bounds the west side of the mountains; this fault is the master fault for the east-tilted, Bosque del Apache half graben (Cikoski, 2010). The Santa Fe Group between the two strands of the LSPMFZ consists of the >50 m thick, early Pleistocene–age Sierra Ladrones Formation unconformably overlying (with angularity) the 700–800 m thick Popotosa Formation. In the Popotosa Formation, an unroofing sequence is recognized by up-section changes in the composition and texture of the conglomerate. Lower strata are characterized by conglomerate clasts dominated by rounded-subrounded limestone with minor, variable percentages of reddish Permian-derived clasts and 1–5% rounded chert. This gravel assemblage closely resembles that of the Eocene Baca Formation. About 50–100 m up-section, Glorieta-derived, reworked sandstone clasts appear, and the gravel becomes slightly more heterolithic; also, intermediate volcanic clasts increase in abundance northwards. In the next overlying 400 stratigraphic meters, red and yellow Permian-derived clasts progressively increase up-section relative to gray limestone clasts, and there is an upward decrease and disappearance of rounded chert and Glorieta Sandstone clasts. Conglomerate in the uppermost 300 m of preserved Popotosa strata is dominated by red and yellow, relatively angular, Permian-derived siltstones and very fine sandstones, which are mixed with minor dolomite and limestone. Age control is provided by a detrital sanidine age of 1.641±0.004 Ma from a pumiceous pebbly sandstone bed in the middle of the Sierra Ladrones Formation and correlation of a >100 m thick basin-floor facies, containing thickly cross-stratified eolianites, to 12–9 Ma strata 6–10 km to the northwest (Cikoski, 2010). We interpret the following exhumational history of the LSPM. In the middle Miocene, the LSPM were low hills capped by the limestone-dominated San Andres Formation, and sediment shed westward into the adjoining Bosque del Apache graben was predominately derived from erosion of the Baca Formation to the east of the LSPM. At 12–8 Ma, displacement rates increased along the east strand of the LSPMFZ, initiating footwall uplift of the LSPM and an eastward shift of basin floor facies toward the immediate hanging wall of that fault. As uplift progressed, lowermost San Andres Formation limestone and Glorieta Sandstone, as well as the underlying Yeso Group, were eroded from these mountains. At the end of the studied Popotosa stratigraphic record, inferred to be 9–7 Ma (but poorly constrained), exposed bedrock in the LSPM was mostly Permian. If one assumes that the readily erodible Permian did not produce notable topographic relief, as is evident by the low topography of Permian strata cropping out in the southern LSPM, then one can use modern topography and the bedrock stratigraphic record to calculate an uplift rate of 53–64 m/my from ca. 7 Ma to 1 Ma. During the Pliocene, extensional strain increasingly shifted to the west strand of the LSPMFZ, resulting in an angular unconformity in the Popotosa Formation between the west and east strands of the LSPMFZ. Based on 15 m of observed vertical displacement of lower-middle Sierra Ladrones Formation strata (2.0–1.0 Ma) and its basal unconformity, throw rates for the east strand of the LSPMFZ were 7.5–15.0 m/my during the Quaternary.

INTRODUCTION

The Little San Pascual Mountains (LSPM) are a small rift-flank uplift located 40 km south-southeast of Socorro, about 9 km southeast of the headquarters of the Bosque del Apache National Wildlife Refuge (Figs. 1, 2). At 8 km long and 2 km wide, and with a relief of only 150–250 m, these mountains are much smaller than many of the larger footwall uplifts of the Rio Grande rift, such as the San Andres, Caballo, Fra Cristobal, Magdalena, or Sandia Mountains. The LSPM are bounded on their west side by the northeast-trending Little San Pascual Mountain fault zone (*sensu* Jochems and Love, 2016), which we abbreviate as LSPMFZ.

During the course of recent STATEMAP geologic mapping work (Koning et al., 2020, 2021), it was discovered that outcrops of both the Popotosa and Sierra Ladrones formations of the Santa Fe Group are present on the northern and western side of the LSPM, separated by an angular unconformity (Fig. 3a). The Popotosa Formation consists of reddish to orangish, tilted sandstone and conglomerate (Fig. 3b–3d). The overlying Sierra Ladrones Formation is composed of tan to light gray, subhorizontal (<3° tilt) strata that can be divided into an axial-fluvial lithofacies assemblage and a west-sloping piedmont lithofacies assemblage (Fig. 3a, unit Qsp).

For the sake of geographic reference, we have informally named canyons draining the western escarpment of the LSPM. They are not formally named on the USGS topographic map. These canyons are (south to north): Coontail, Andesite, Fox, and Red House canyons (Fig. 2). Another informal landmark is "Chert hill" at the north end of the mountains (Fig. 2).

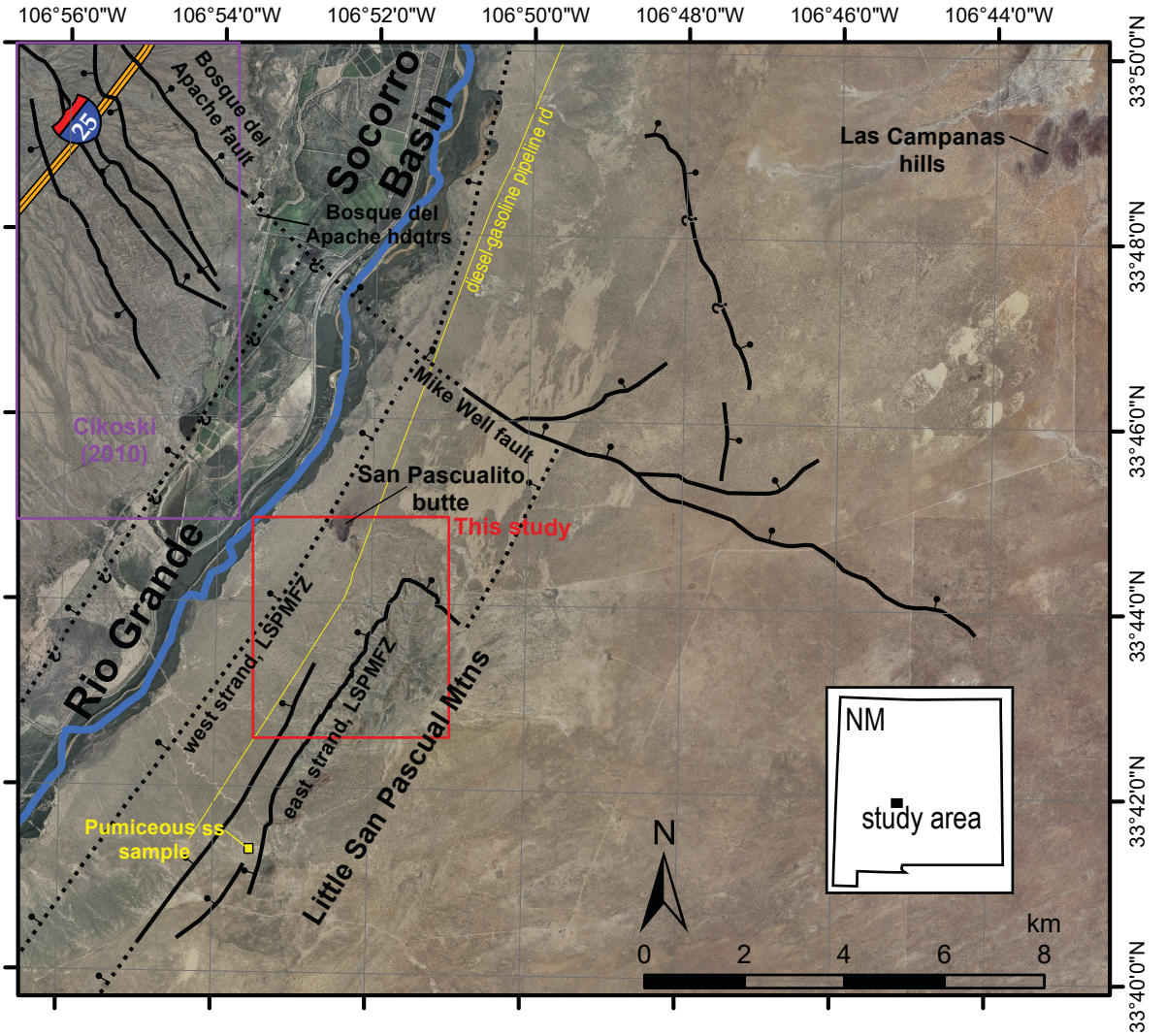

FIGURE 1. Location of study area (red rectangle) and the study area of Cikoski (2010; purple rectangle) shown on a LANDSAT image base. Major faults are depicted by thick black lines (ball-and-bar on down-thrown side). LSPMFZ = Little San Pascual Mountain fault zone.

PURPOSE

The purpose of this paper is to describe the sedimentologic and stratigraphic features of the Popotosa Formation, as well as the extensional strain (i.e., tilting, throw rates on faults) that has deformed it. We particularly focus on up-section changes that occur in sedimentologic texture, composition, and paleocurrent data. Clast composition and texture of conglomerates in the Popotosa Formation are compared to that observed in underlying and overlying formations as well as the nearby bedrock stratigraphy of the LSPM. Using these data, we interpret the exhumational (uplift) and faulting history associated with the Little San Pascual Mountain fault zone for the middle Miocene through Quaternary.

PREVIOUS WORK

Only two previous geologic studies have been undertaken on the LSPM, both focused on the Pennsylvanian–Permian bedrock that composes the range (Geddes, 1963a, 1963b; Lucas et al., 2017). Geddes (1963a, b) discovered that the general structure of the mountains corresponds to an anticline trending 030°. A stratigraphic section measured by Lucas et al. (2017) and recent mapping (Koning et al., 2020, 2021) indicate that the Pennsylvanian section is 700 m thick and comprised of the Red House, Gray Mesa, and Bar B formations (Fig. 4). These relatively limestone-rich Pennsylvanian strata underlie the northern, higher-elevation part of the range. The southern, lower-elevation part of the range features a relatively contiguous section of 800 m thick Permian strata that strike northeast and dip southeast. More information about the bedrock stratigraphy can be found in Lucas et al. (2017) and Koning et al. (2020, 2021).

An excellent sedimentologic-stratigraphic study has been done on Popotosa Formation outcrops located 6–10 km to the northwest, on the west side of the Rio Grande. In that locality, detailed mapping of the Popotosa Formation allowed development of a stratigraphic scheme based mainly on sediment texture and gravel composition (Cikoski, 2010; Chamberlin and Cikoski, 2010). Provenance and paleocurrent data,

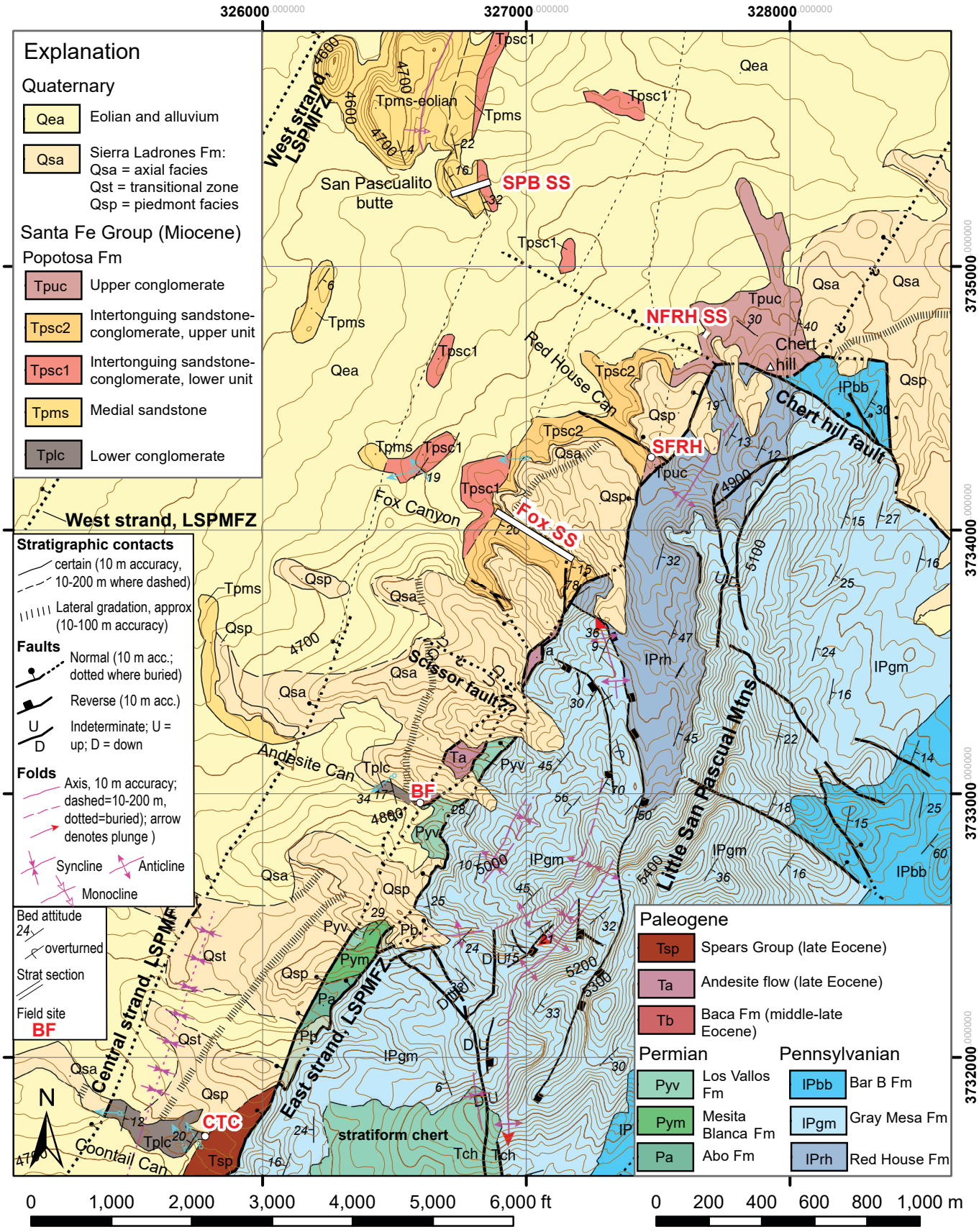

FIGURE 2. Geologic map of study area (red rectangle of Fig. 1) simplified from the geologic maps of Koning et al. (2020, 2021) and modified according to observations made in the Fall of 2021. Key field sites are labeled in red and are abbreviated as CTC = Coontail canyon, BF = Baca Formation, SFRH = South Fork of Red House canyon, NFRH SS = North Fork of Red House Canyon stratigraphic section (Fig. 9), Fox SS = Fox Canyon stratigraphic section (Fig. 8), and SPB SS = San Pascualito Butte stratigraphic section (Fig. 7). Important faults are labeled in black text, where LSPMFZ = Little San Pascual Mountain fault zone.

combined with age control provided by an oreodont fossil and dated pumice, indicate that the depositional environment at 15–8 Ma consisted of a southwestward-sloping piedmont developed in a southeast-tilted graben. This graben, called the Bosque del Apache graben, was tilted toward faults that continued northward from the base of the LSPM. Gravelly piedmont sediment at 12–9 Ma interfingered south-southwestward with eolian deposits featuring meter-scale cross stratification. The piedmont sediment consists of two petrosomes sourced from the northeast. The northern petrosome is characterized by a rhyolitic ignimbrite volcanic assemblage and the southern by an intermediate ± ignimbrite-dominated volcanic assemblage. Eolian deposits are not found in the oldest stratigraphic units, one of which has 14.59±0.05 Ma pumice clasts. The oreodont fossil (11–9 Ma; Morgan et al., 2009) was found in the interbedded eolian-conglomeratic strata. Based on the stratigraphic correlation chart of Cikoski (2010, Fig. 11), eolian deposits appear to be constrained to ca. 12–9 Ma.

METHODS

During mapping of the Little San Pascual Mountain quadrangle (Koning et al., 2021) and San Marcial quadrangle (Koning et al., 2020), all outcrops of the Popotosa and Sierra Ladrones formations were described in detail using standard geologic procedures. These descriptions included visual estimation of the percentage of conglomerate-clast (gravel) composition and sizes (i.e., pebble [2–64 mm] vs. cobble [64–256 mm] vs. boulder [>256 mm], following Wentworth, 1922, but note that "granules" are lumped with the pebble-size fraction).

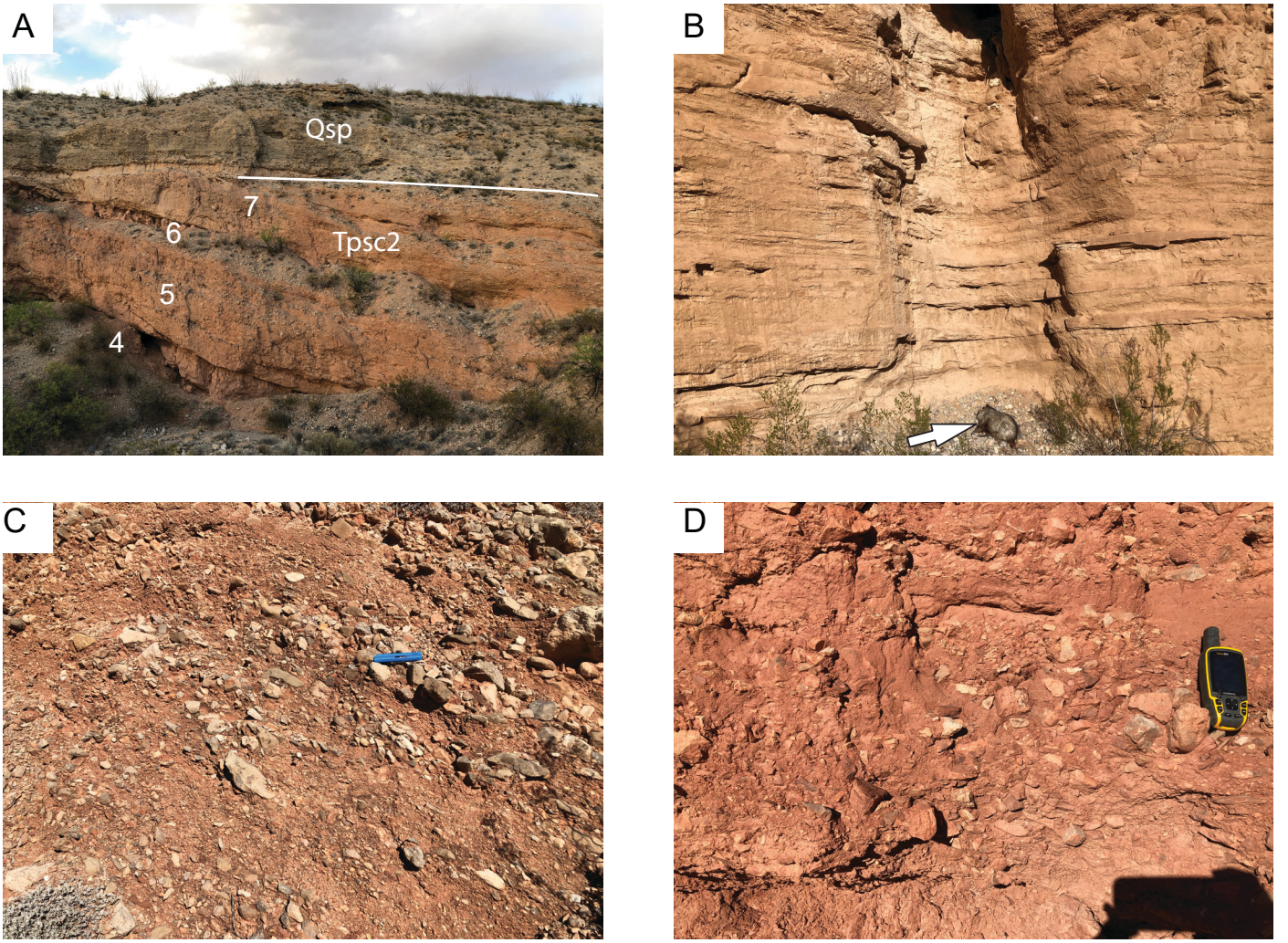

FIGURE 3. Photographs illustrating the Popotosa Formation. Photos A–C show the upper subunit of the intertonguing sandstone-conglomerate unit (Tpsc2), and Photo D illustrates the upper conglomerate unit (Tpuc). (A) Angular unconformity between the piedmont facies of the Sierra Ladrones Formation (Qsp) and this unit of the Popotosa Formation (Tpsc2). In the latter, note the alternation of conglomeratic intervals and recess-forming sandstone intervals; white numbers are units described in the Fox Canyon stratigraphic section (Fig. 8, Appendix 2). (B) Close-up of basin floor facies in Tspc2; note the thin-medium, tabular to wedge-shaped beds that are composed mainly of fine-grained sandstone. Dead javelina at base of exposure (white arrow) is about 1 m long. (C) Conglomeratic interval illustrating gravelly alluvial fan facies (unit 11 of the Fox Canyon stratigraphic section, Fig. 8, Appendix 2); note the tabular to lenticular bedding and lack of cross stratification, consistent with relatively unconfined flow. Blue ruler is 15 cm long. (D) Debris flow facies of unit Tpuc adjacent to the east strand of the LSPMFZ in the lower part of the upper conglomerate unit (labeled as site SFRH in Fig. 2). Note the matrix-supported, relatively massive appearance of the gravel, the angularity of the clasts, and the high proportion of reddish-brown, Permian-derived clasts. These features strongly suggest proximal deposition by a high proportion of debris flows, compared to less-dense (less muddy) stream-flow deposits, on an alluvial fan adjacent to a paleotopographic high.

Sand color and grain size were respectively measured in the field using a Munsell color chart and grain-size card. Note that the term "conglomerate" is used when referring to relatively consolidated or indurated, meter-scale stratigraphic units or features, whereas individual, gravel-size clasts are referred to interchangeably as "conglomerate clasts," "clasts," or "gravel."

After mapping was completed, three stratigraphic sections were measured in well-exposed areas using a Jacob staff and Abney level. These stratigraphic sections are called San Pascualito Butte, North Fork Red House Canyon, and Fox Canyon (locations shown in Fig. 2). For the conglomeratic intervals in and outside of the stratigraphic sections, paleoflow was measured using gravel imbrication and clast counts made to determine gravel composition. Paleoflow measurements were adjusted in areas of steep stratal tilts (>20°) in the following manner. Bedding orientations closest to each site were used to restore imbricated gravel positions back to horizontal using the program Stereonet (Allmendinger et al., 2012; Cardozo and Allmendinger, 2013). Paleoflow data were input as lines, with bearing (trend) being the direction of imbrication and plunge being the maximum dip value of the clast. Given that imbrication records paleoflow in the up-dip direction (i.e., opposite of what was measured), we then converted the restored bearing values to the paleoflow direction by adding 180°. In the Fox Canyon stratigraphic section, the maximum clast size was

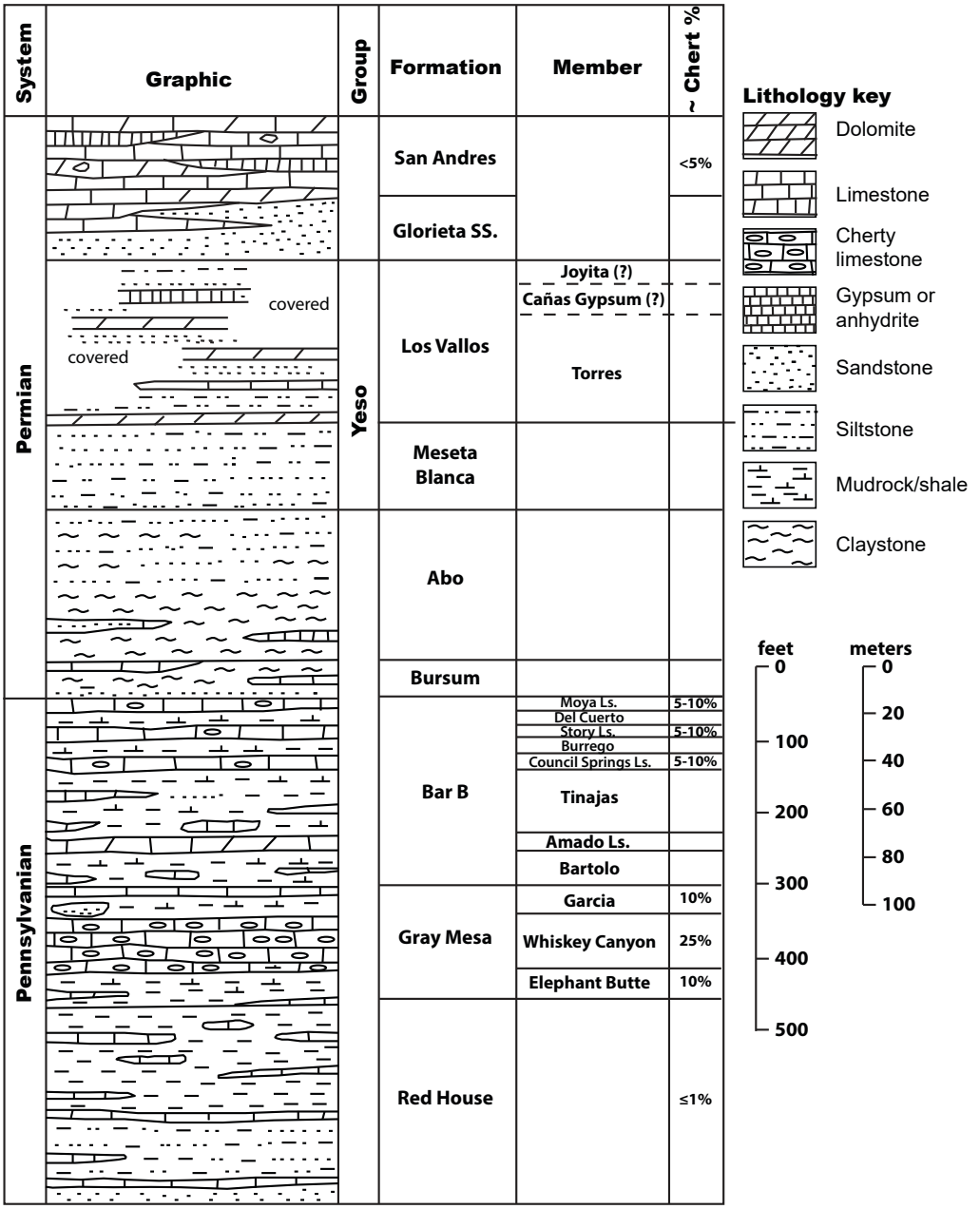

FIGURE 4. Stratigraphic column of the bedrock stratigraphy of the Little San Pascual Mountains, based on the mapping of W. John Nelson and Scott Elrick (Koning et al., 2021). We chose the Pennsylvanian nomenclature of the Truth or Consequences area to be consistent with the earlier study here by Lucas et al. (2017). Figure courtesy of Scott Elrick.

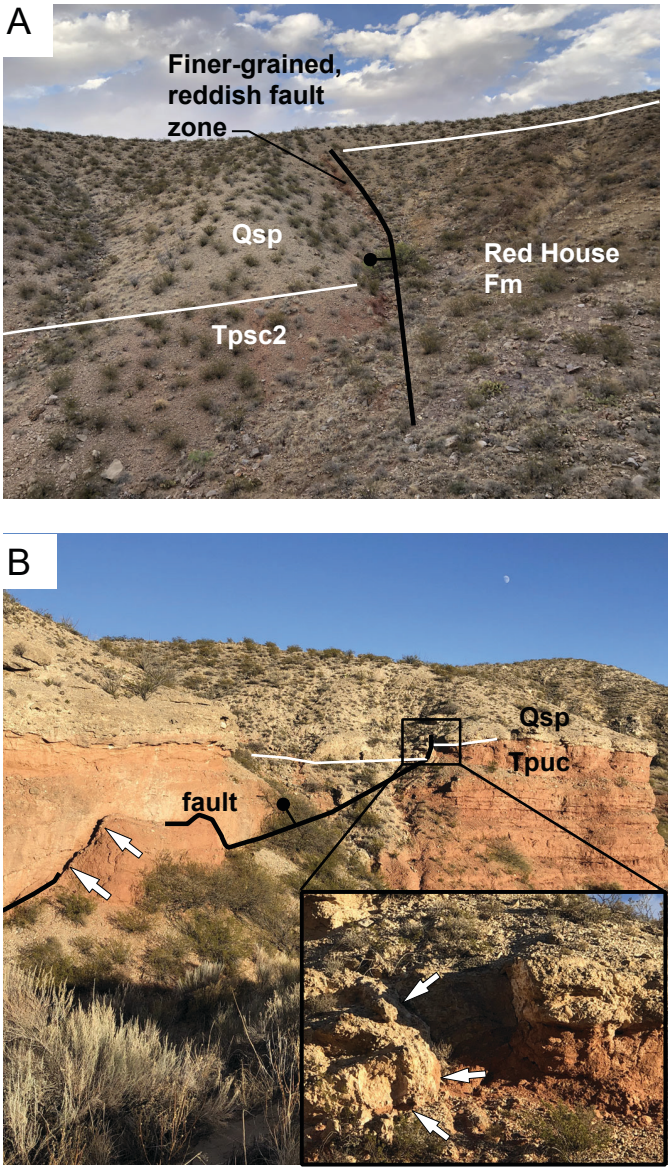

FIGURE 5. (A) Photograph of the east strand of the Little San Pascual Mountain fault in Fox canyon, view to north. Pennsylvanian Red House Formation on the footwall, which has been onlapped by the piedmont facies of the Sierra Ladrones Formation (Qsp). The upper unit of the intertonguing sandstone-conglomerate map unit (Tpsc2) lies below Qsp on the hanging wall. Note the reddish, fine-grained sediment in the fault zone only ~5 m below the upper surface of Qsp, inferred to have been derived from Permian red-bed sediment incorporated into the fault zone (a wider sliver of these red beds is present near where the photo was taken). The presence of this fine-grained sediment indicates the contact is not a sedimentologic buttress relation; if the fine-grained sediment was at the surface, as a steep slope before burial by Qsp, it likely would have been completely eroded. The 15 m of vertical separation of the Sierra Ladrones basal contact (white line) indicates fault throw since deposition of lower-middle Sierra Ladrones strata inferred to be 2.0–1.0 Ma (see text for age control). (B) Photograph of a northwest-striking fault offsetting the Santa Fe Group. The thick black line corresponds to a northwest-striking fault, one of two directly observed to have offset the Popotosa Formation (here, the upper conglomerate map unit). Where not annotated by black line, white arrows point to fault location. This northwest-striking fault set also has offset bedrock strata in the Little San Pascual Mountains and is present on the west side of the Rio Grande (Cikoski, 2010; Chamberlin and Cikoski, 2010). The fault exhibits down-to-the-northeast throw. Inset panel (lower right) shows 1 m of displacement of the unconformity between the Sierra Ladrones Formation and the Popotosa Formation. In Fox canyon, another northwest-striking fault has vertically offset the same contact by 2–3 m.

measured with a ruler in the field.

$^{40}Ar/^{39}Ar$ analysis was conducted on a pumice-rich sand sample called SM-596-200319. Individual sanidine crystals were extracted from the sand. Eighteen single crystals were dated using a Thermo-Fisher Scientific ARGUS VI mass spectrometer for argon isotopic analysis. Argon was extracted by heating with a CO_2 laser with a heating time of 30 seconds followed by gas cleanup for 30 seconds using SAES NP-10 getters. Complete methods of sanidine geochronology is outlined in Heizler et al. (2021), and specific information for this sample is provided in the footnotes of the data table in Appendix 1.

RESULTS

Structure

Recent geologic mapping (Koning et al., 2020, 2021) indicates that there are two large-displacement strands of the LSPMFZ, called the east and west strands (Fig. 2). Both strands strike 035° and exhibit west-down throw (each with likely several hundred meters to perhaps >1 km of inferred throw). In between is a central strand that appears to terminate to the north (Fig. 2).

The east strand of the LSPMFZ makes an abrupt ~90° turn at the northwest corner of the mountains (Fig. 2). At this turn, another fault branches off to the northwest at a 322° strike and 48–63°NE dip, presumably exhibiting northeast-side-down dip-slip. Southeast of the bend, Koning et al. (2021) mapped a northwest-striking, northeast-down normal fault that bounds the northern end of LSPM—informally named the "Chert Hill fault" because of local hill-forming silicification in its immediate hanging wall (Fig. 2). South of the bend, the east strand of the LSPMFZ exhibits a sinuous trace and there is a 2 km long, 100–200 m wide, fault-bounded sliver of northwest-dipping Permian strata (Fig. 2). Near the north end of this fault-bounded sliver, a northwest-striking scissors fault (labeled as such in Fig. 2) is inferred that separates east-dipping strata (to the north) from west-dipping strata (to the south). An important observation regarding timing of motion along the east strand of the LSPMFZ is found in Fox canyon immediately adjacent to the fault. Here, lower Sierra Ladrones strata and its basal unconformity are offset 15 m by the fault (Fig. 5a). The presence of easily erodible, fine sediment in the fault zone (presumably from Permian strata due to its red color) indicates a faulted juxtaposition rather than a stratigraphic buttress unconformity. If the latter were the case, this fine-grained, fault zone material would have been eroded away due to exposure on a steep, subaerial topographic slope.

Northwest-striking faults offset the Popotosa Formation in two exposures (Fig. 5b); there are likely more in poorly exposed areas. These faults have the same strike (310°) as a set of dip-slip faults observed in the bedrock of the LSPM (Fig. 2). The Popotosa Formation is vertically offset several meters, in a normal sense, by these northwest-striking faults. The overlying Sierra Ladrones Formation is offset 1 m on the northern of these faults (in Red House canyon; SFRH in Fig. 2) and 2–3 m on the southern of these faults (in Fox canyon; Fig. 5b).

The northwest-striking Chert Hill fault, bounding the north end of the LSPM, has much more throw (est. 0.5 km) than other faults in the northwest-striking fault set. Based on provenance and paleocurrent data of the Popotosa Formation (discussed below), the Chert Hill fault likely links with another northeast-striking, west-down fault that exposed Abo–lower Yeso Group strata in its footwall during the late Miocene (dotted fault in upper right corner of Fig. 2).

Lithologic Units

The spatial distribution of lithologic units is shown in the geologic map of Figure 2, which also shows the bedrock geology. A simplified diagram of stratigraphic relations is presented in Figure 6. The sedimentologic properties of the lithologic units are documented in a variety of datasets. Description and thickness details of the stratigraphic sections are in Appendix 2 and clast composition in Appendix 3. Graphic columns for the three stratigraphic sections in the Popotosa Formation are depicted in Figures 7–9. Figure 10 graphically illustrates conglomerate clast compositions for various sites in the Popotosa Formation; because their gravel-clast composition is important for exhumation and paleogeographic interpretations, we also include these data for both the Baca and Sierra Ladrones formations in Figure 10 and Appendix 3.

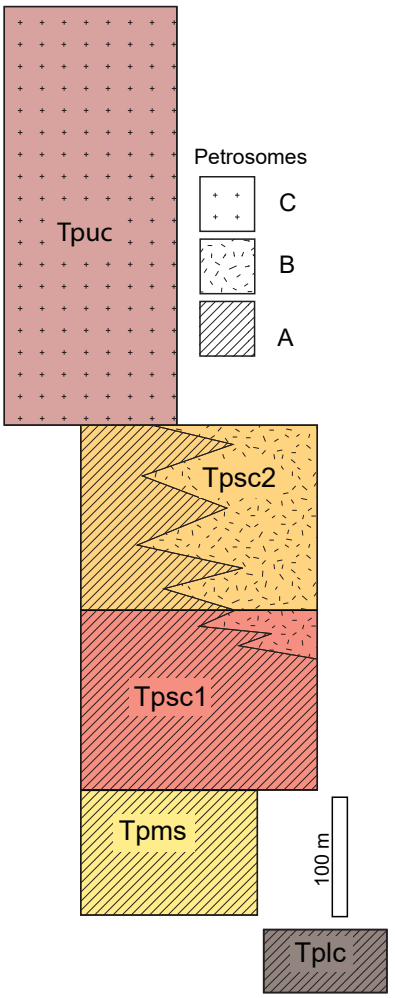

FIGURE 6. Schematic stratigraphic chart showing thickness of the Popotosa Formation map units and the position of the gravel petrosomes relative to these map units. The geologic symbols are defined in Figure 2. Petrosome A is characterized by rounded-subrounded limestone with minor, but variable, percentages of reddish, Permian-derived clasts and 1–6% rounded chert. Petrosome B is characterized by the presence of Glorieta-derived, reworked sandstone clasts mixed with limestone and Permian-derived clasts. Petrosome C is composed exclusively of Permian-derived clasts. North is to the left.

In the following, we categorize gravel composition into four petrosomes (Fig. 10, Appendix 3). Petrosome A clasts are typified by rounded limestone, subordinate and variable percentages of reddish siltstone–very fine sandstone derived from Permian strata, trace–6% rounded chert, 0–4% green to olive-colored quartzose sandstone, and 0–3% presumed Glorieta Sandstone. What we refer to as Glorieta Sandstone clasts consist of yellow-tan, fine-lower to medium-upper sand-grain size, quartzose sandstone that looks similar to the Glorieta Sandstone exposed in the southernmost LSPM. We acknowledge that some Cretaceous sandstones, particularly the Gallup Sandstone or the Tres Hermanos Sandstone, may have a similar appearance. However, in the larger region (including the Carthage area), the exposed Glorieta Sandstone is the closest and the more indurated, so we infer that most of the sandstone of this type most likely is from the Glorieta Sandstone. Petrosome B clasts are typified by limestone and subordinate reddish (as well as minor yellow), siltstone–very fine sandstone derived from Permian strata. There is no rounded chert, and the limestone clasts are angular to subrounded. Petrosome C is characterized by a predominance of red to yellow, Permian-derived clasts. Petrosome D is restricted to the piedmont facies of the Sierra Ladrones Formation. The gravel here is dominated by angular-subangular limestone with minor (1–5%) brownish-greenish sandstones (locally micaceous or arkosic) and 5–10% angular, typically reddish-brown chert.

Baca Formation

The Baca Formation is present in three places west of the LSPM, only one of which lies in the geologic map of Figure 2 (label BF in Andesite canyon). To the south, the Baca Formation directly overlies the upper Yeso Formation (Koning et al., 2020). The Baca Formation consists of meter-scale, intercalated tongues of (1) reddish-brown, massive, very fine– to fine-grained sand and silty-clayey fine sand, (2) gray, fine- to medium-grained sand composed of feldspar, quartz, and lithic fragments, and (3) conglomerates and conglomeratic sandstones. South of the area shown in Figure 2, Baca Formation conglomerates consist of pebbles with ~10% cobbles and 1–5% boulders that are composed of rounded, Paleozoic limestone, 1–3% reddish-brown siltstone–very fine sandstone (derived from Permian strata), and 1–5% rounded chert (Fig. 10 and Appendix 3, SM-571c). Paleoflow was toward the east.

The Baca Formation also occurs at site "BF" in the study area (Figs. 2, 11a). Here, a minor proportion of Baca strata consist of ledge-forming, thick, steeply dipping conglomerate beds (253°, 53°NW) that are conformably overlain by an andesitic flow. Compared to the southern Baca Formation sites, this conglomerate is notably coarser (more cobbly-bouldery) and

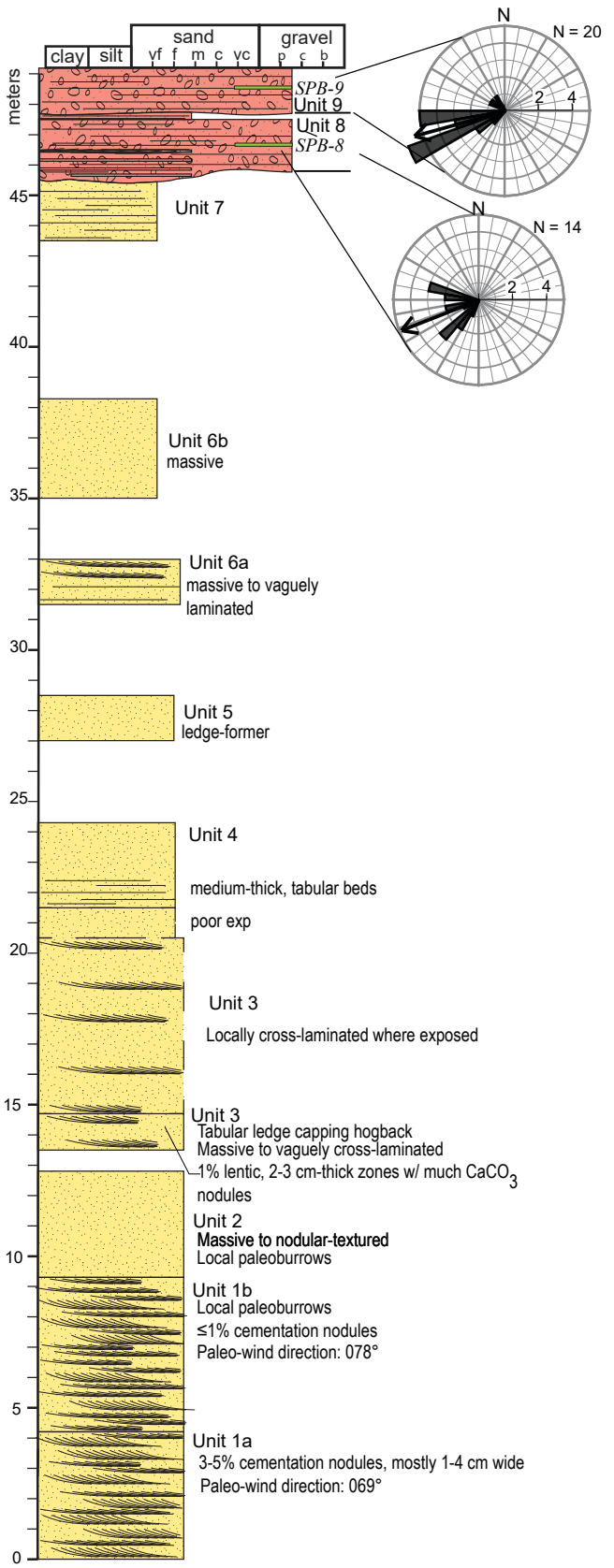

FIGURE 7. San Pascualito Butte stratigraphic section, located on east side of San Pascualito Butte (white line and SPB SS label on Fig. 2). Paleoflow from clast imbrication is plotted on rose diagrams next to the graphic column. Italicized font adjoining green rectangles are clast-count sites (Appendix 3, Fig. 10).

contains a higher proportion of reddish-brown Permian clasts (19–35%; Appendix 3, Figs. 10, 11a). All of the conglomerate clasts for the Baca Formation are classified as Petrosome A.

Popotosa Formation

The Popotosa Formation occurs in relatively small and discontinuous, albeit well-exposed, outcrops west of the east strand of the LSPMFZ and north of the Chert Hill fault (Fig. 2). There is a possibility of concealed structures between these outcrops. However, the apparent lack of repeated strata between outcrops north of the inferred scissor fault (Fig. 2) suggests that any such buried faults have relatively minor throw (assuming these faults are northwest-down like the east strand of the LSPMFZ). Four map units of the Popotosa Formation are differentiated (labels given in parentheses): (1) lower conglomerate (Tplc), (2) medial sandstone (Tpms), (3) intertonguing sandstone and conglomerate (Tpsc1 and Tpsc2), and (4) upper conglomerate (Tpuc; Fig. 6). The conglomeratic intervals are interpreted as being associated with an alluvial fan depositional environment based on the dominance of gravel, the presence of thin to medium, tabular to lenticular beds, and the lack of cross stratification that are consistent with high-energy sheet flooding (Fig. 3c). Most of the gravel in the alluvial fan facies is inferred to have been deposited by streamflow processes, because the gravel is mostly clast supported, well-bedded, lacking in fines, and imbrication is well-defined. However, at the base of the upper conglomerate are inferred debris-flow beds (Fig. 3d). The depositional environment of the sandstone-dominated strata is detailed below.

Lower conglomerate lithosome (Tplc)

The lowest Popotosa Formation is characterized by strongly cemented, conglomeratic strata containing rounded-subrounded gravel correlated with Petrosome A. Conglomerate clasts are comprised of very fine to very coarse pebbles, 10–30% fine to coarse cobbles, and trace to 5–10% boulders. Conglomerate composition is correlated to Petrosome A because it is dominated by limestone with 1–10% reddish-brown, Permian-derived clasts, 0–1% Glorieta Sandstone, and 0–6% rounded chert (Fig. 10). Locally, there are up to 2% quartz and 2% other sandstone clast types (Appendix 3) and up to 20% sandstone interbeds that are reddish-yellow and medium to thick-bedded, wedge-shaped, and internally massive. Measured paleoflow is to the west-northwest in Coontail canyon (south edge of Fig. 2), but to the north (in Andesite canyon) paleoflow is to the southwest.

Medial sandstone lithosome (Tpms)

Close to the diesel-gasoline pipeline road, Popotosa Formation strata consist of >130 m thick, relatively well-sorted, reddish-brown to red, very fine– to medium-grained sandstone (mostly fine- to medium-grained) that is mapped as the "medial sandstone." This unit conformably underlies Tpsc1 (Fig. 6). The basal contact of the medial sandstone unit is not exposed.

The lower ~100 m of this unit consists of a reddish-brown sandstone characterized by tangential foresets that are up to 3 m thick within very thick, tabular beds (Figs. 6, 7). Several measurements of foreset strikes and dips indicate a consistent northeast dip. Tabular beds become thinner (10 cm to 1.5 m) and thick cross stratification disappears up-section, the latter replaced by vague, low-angle cross-laminations, horizontal-planar laminations, or massive textures. Locally, paleoburrows are evident.

The depositional environment of this map unit is interpreted as basin floor. Gravel is lacking and strata are characterized by fine- to medium-grained sand that is well sorted and subrounded-rounded. Eolian facies is found down-section and to the north (near San Pascualito Butte, Fig. 2, labeled as Tpms-eolian) based on the 3 m thick cross stratification sets, where foreset dips indicate a northeast-directed paleowind direction. Up-section and to the south, the paleodepositional environment is interpreted as eolian sand sheets reworked by sheetflooding.

Intertonguing sandstone-conglomerate lithosome, lower unit (Tpsc1)

The lower unit of the intertonguing sandstone-conglomerate map unit is characterized by tabular-bedded, reddish-brown sandstone interbedded with subordinate conglomerates. The conglomerates occur in tabular intervals at least a few meters thick. Conglomerates consist of subrounded gravel (ranging from angular to rounded) comprised of pebbles with 10–15% fine to coarse cobbles. Gravel composition fits with Petrosome A and is as follows (Appendix 3, Fig. 10): 64–89% limestone with 3–40% reddish Permian clasts, 0–4% rounded cherts, 2–3% Glorieta Sandstone, and 0–4% greenish to brownish, fine- to medium-grained sandstone clasts (resembling Crevasse Canyon Formation sandstones). At two sites, 1–2% granite clasts were observed (e.g., uppermost conglomerate of the San Pascualito Butte stratigraphic section [clast count SP-9, Fig. 7, Appendix 3]). Paleoflow was mainly to the west-northwest.

A particularly important observation in this unit is the northward increase in the percentage of volcanic gravel. These are mostly andesitic (often plagioclase-phyric), but trace porphyritic ignimbrite clasts were also observed. These volcanic clasts are negligible (i.e., locally trace amounts are observed) near Fox canyon, but the proportion increases northwards to as much as 20–50% near the northern study area boundary east of San Pascualito Butte (e.g., unit 8 in the San Pascualito Butte stratigraphic section, sites SP-8 and SP-9 in Figs. 7 and 10).

Intertonguing sandstone-conglomerate lithosome, upper unit (Tpsc2)

The upper unit of the intertonguing sandstone and conglomerate (Tpsc2) is well-illustrated in the Fox Canyon stratigraphic section (Fig. 8). The lower contact is gradational with the lower sandstone-conglomerate (Tpsc1) and difficult to map at 1:12,000 scale. This unit is characterized by relatively thick tongues (each tongue being a few to several meters thick) of conglomerate and sandstone. The sandstone color is more or-

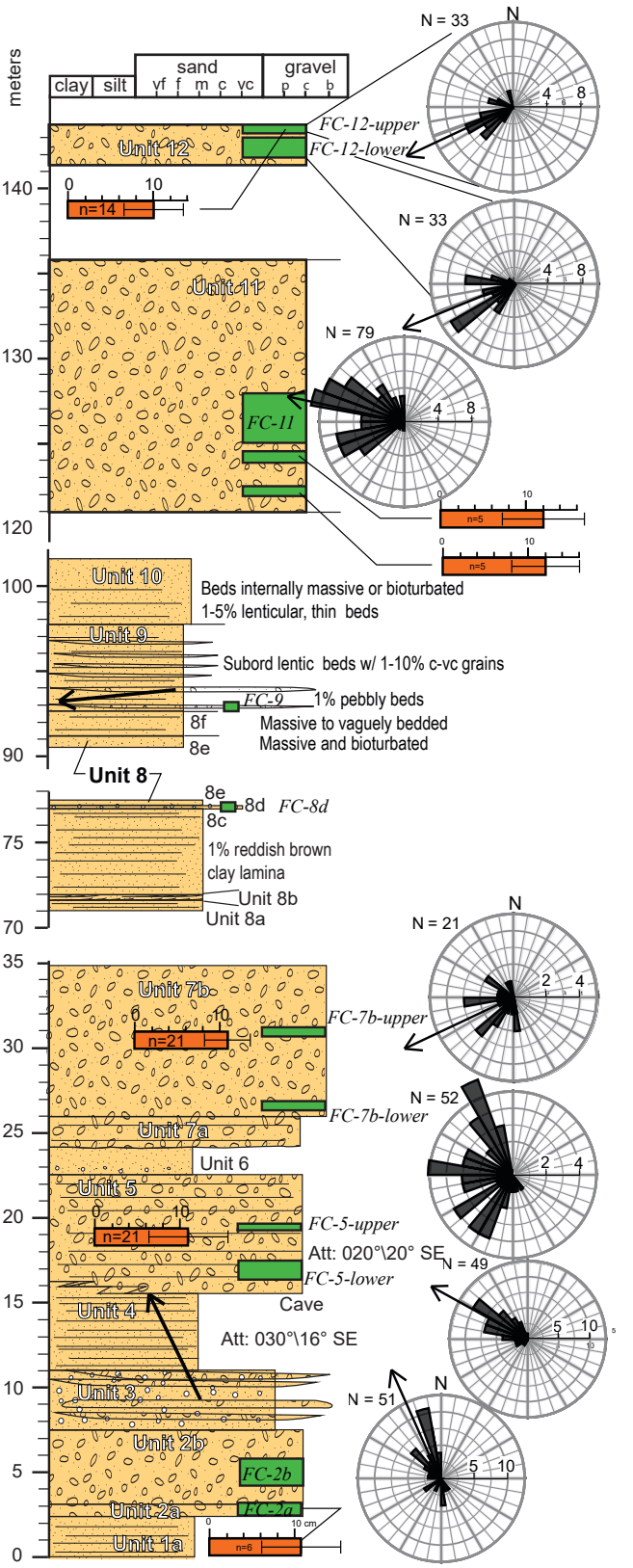

FIGURE 8. Fox Canyon stratigraphic section (Fox SS on Fig. 2). Paleoflow from clast imbrication is plotted on rose diagrams next to the graphic column. Average of maximum clast size is shown by the orangish-tan bar, with the brackets denoting one standard deviation. Italicized font adjoining green rectangles are clast-count sites (Appendix 3, Fig. 10). Single black arrows on the graphic column denote paleoflow determined using <15 clasts; north for this representation is to the top of the page.

ange and less reddish than that observed in the lower sandstone unit.

Sandstone strata are in well-defined, very thin to medium, tabular beds locally separated by 1–7% lamina of silt or clayey-silty, very fine–fine sand; up to 5% of sand bodies are lenticular (Fig. 3b). The sand is mostly very fine– to medium-grained, subrounded-subangular, and composed of quartz, minor feldspar, and 1–5% sedimentary-lithic grains (based on hand-lens inspection). Within these sandstone strata are very sparse beds of pebbly sandstone (Fig. 8, FC-8d and FC-9), where the pebbles are subangular to rounded and contain the following lithologic types: rounded limestone; 2–5% rounded chert; 1–5% yellowish, very fine–grained, and quartzose sandstone; 1–3% greenish, quartzose sandstone; 1–5% reddish, Permian-derived clasts; and trace–1% granite(?) (Fig. 10, FC-8d and FC-9). This clast composition correlates with Petrosome A, and the highest observed stratigraphic level of this petrosome is in the Tpsc2 unit. Imbrication of four clasts indicate a 264° paleoflow direction (Fig. 8, single arrow at the base of unit 9).

Conglomeratic intervals are composed of the Petrosome B suite. Gravel is primarily pebble-size, with 1–20% cobbles and 0–3% boulders, and it is clast- to sand-supported. There is no obvious up-section trend in clast sizes (Fig. 8), but clasts become less rounded (more angular) up-section (Fig. 10). Gravel composition is dominated by limestone (Fig. 10, Appendix 3). The proportion of reddish-brown, Permian clasts progressively increases up-section at the expense of limestone gravel. There are also a few percent yellowish to light gray, very fine–grained, quartzose sandstones and siltstones similar to those seen in the Los Vallos Formation; this gravel type increases up-section in the Fox Canyon stratigraphic section (Fig. 10, FC-2a through FC-12). Importantly, there is an upward disappearance of Glorieta sandstone clasts in the Fox Canyon section (Fig. 10, FC-2a through FC-12). Although difficult to quantify, in an up-section direction, the carbonate clasts become increasingly dolomitic, tannish, and micritic—resembling carbonate types seen in the Torres Member of the Los Vallos Formation.

The tabular-bedded sandstone tongues are interpreted to have been deposited by alluvial sheet flooding on a basin floor. The sand is relatively well sorted, the beds lack cross stratification, and locally silt or clayey to silty very fine–fine sand occur as lamina between thicker beds. The sparse gravel lenses within the sandstone tongues are distinct in composition (Petrosome A) from that in the adjoining conglomeratic, alluvial fan tongues (Petrosome B) and have a different provenance.

Upper conglomerate lithosome (Tpuc)

The upper conglomerate is characterized by relatively angular gravel that belongs to Petrosome C. This map unit is illustrated by strata described in the North Fork of Red House Canyon stratigraphic section (Fig. 9). Gravel is mostly clast-supported, poorly sorted, imbricated, and subangular-angular. Conglomerate clasts are mostly pebble-size with 5–10% cobbles. Beds commonly alternate between those dominated by clasts of yellowish siltstones to very fine sandstones and yellowish-tannish dolomites versus beds dominated by reddish-brown,

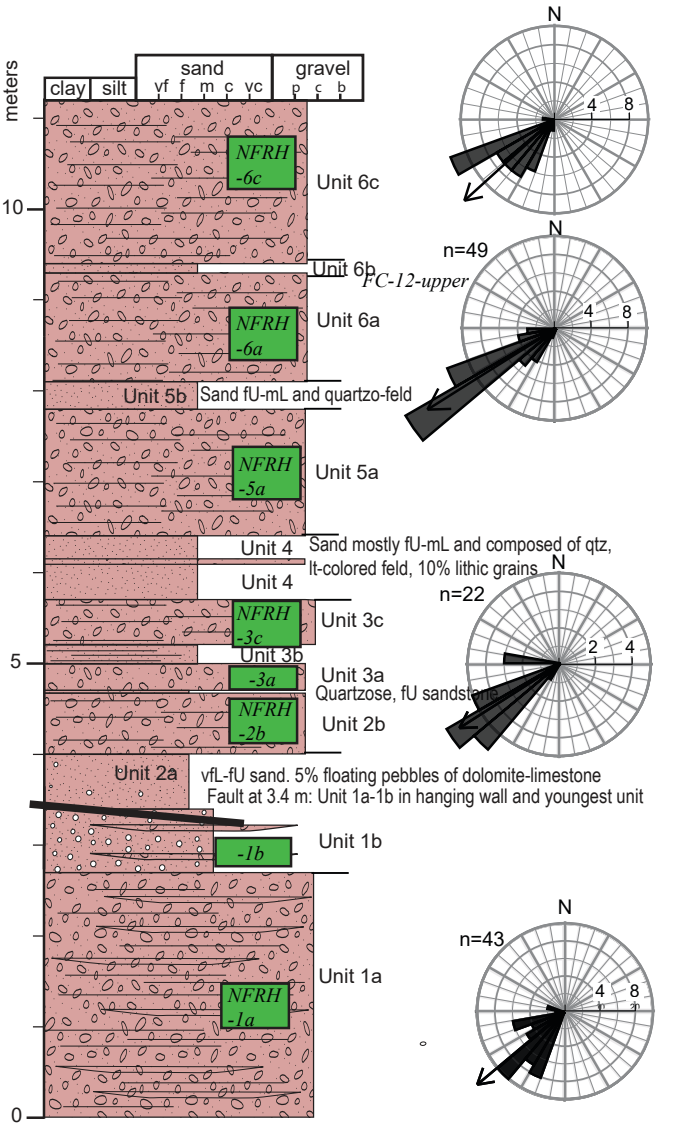

FIGURE 9. North Fork of Red House Canyon stratigraphic section. Paleoflow from clast imbrication is plotted on rose diagrams next to the graphic column. Italicized font in the green rectangles are clast-count sites (Appendix 3, Fig. 10). A fault was encountered in the lower part of the section, interpreted to be west-down and resulting in the youngest stratigraphic unit being on the hanging wall (unit 1a and unit 1b).

Permian-derived clasts. The percentage of limestone is <25% (Fig. 10). The stratigraphically highest strata, observed on the hanging wall of a fault (units NFRH-1a and NFRH-1b, Fig. 9) consist totally of reddish-brown, Permian-derived clasts. There are minor beds, up to 0.2–0.7 m thick, composed wholly of relatively well-sorted, very fine– to medium-grained sandstone composed mostly of quartz grains. Debris flow facies is interpreted adjacent to the east strand of the LSPMFZ in the South Fork of Red House canyon (SFRH, Figs. 2, 3d).

Sierra Ladrones Formation (piedmont facies)

The Sierra Ladrones Formation consists of an axial-fluvial facies to the west that intertongues with a piedmont facies to the east. The piedmont facies is characterized by tabular to broadly

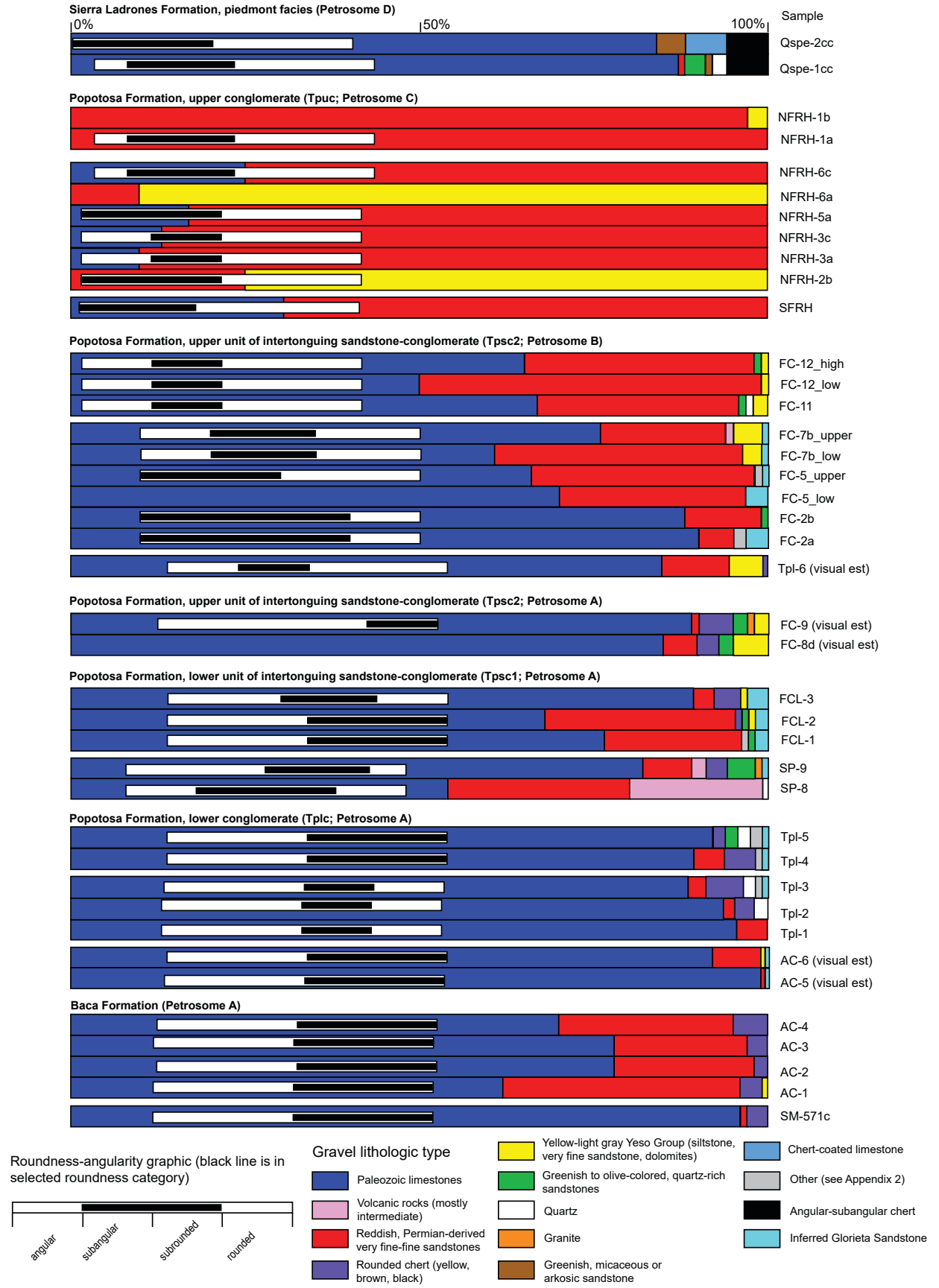

FIGURE 10. Bar graphs illustrating gravel composition data for the Baca, Popotosa, and Sierra Ladrones (piedmont facies) formations. The Popotosa Formation is differentiated according to map unit and gravel petrosome. Black shading with the narrow white rectangle denotes gravel roundness. See explanation at the base of the figure for the gravel-roundness bar and the gravel lithologic type.

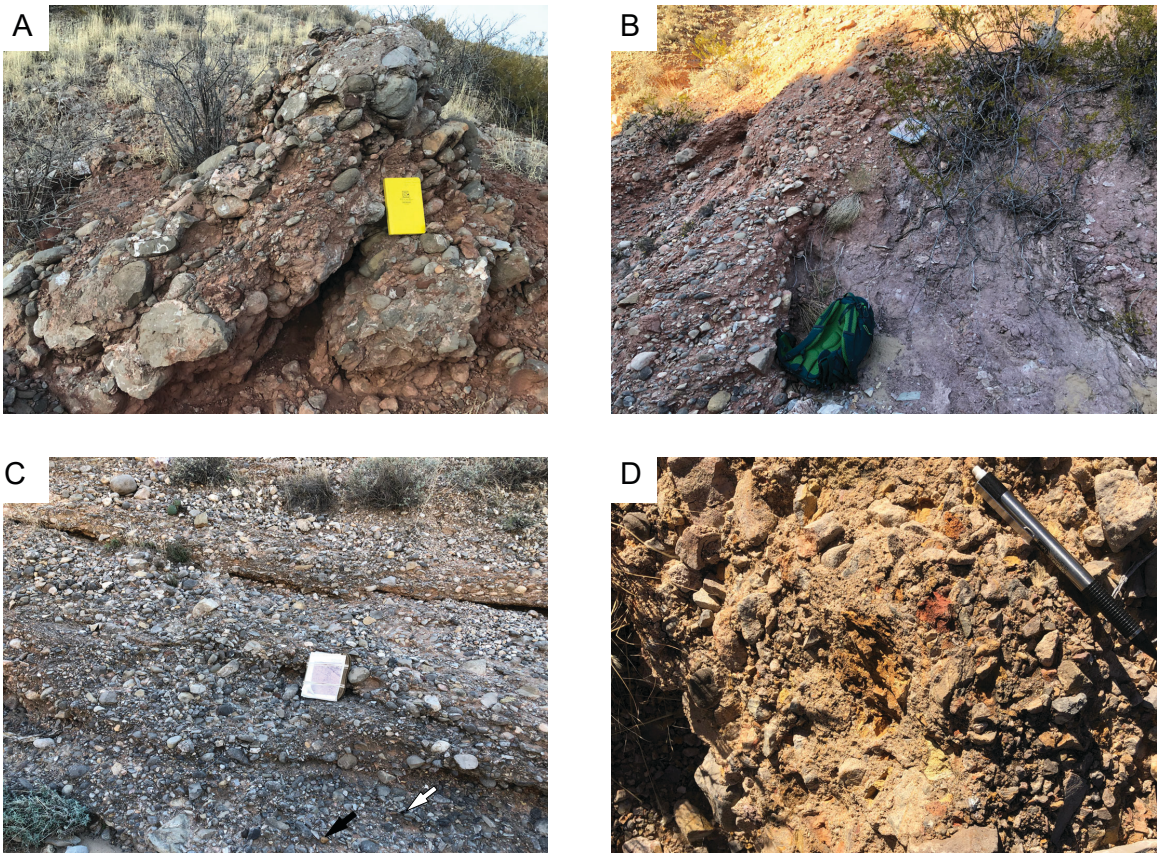

FIGURE 11. Photographs of the Baca Formation compared to the lower conglomerate map unit of the Popotosa Formation. (A) Baca Formation is tilted steeply to the left (west) at site BF (labeled in Andesite canyon on Fig. 2); view to north. Note the high proportion of cobbles and the rounded nature of the gravel, which consists of limestone and subordinate reddish, Permian-derived clasts. (B) Basal strata of the lower conglomerate buttressed against purplish Spears Group (late Eocene) at site CTC in Coontail canyon (Fig. 2). The lower conglomerate clearly filled a paleovalley. Map board and backpack are placed on the contact; view to north. (C) Lower conglomerate about 40–50 m (estimate) above the base of the unit. Note the rounded texture of the clasts. White arrow points to a black chert clast, and the black arrow points to a yellow fine- to medium-grained, quartzose sandstone interpreted to be Glorieta Sandstone. The majority of the clast types are gray limestone with only 1–5% reddish, Permian-derived clasts; view to south-southeast. (D) A markedly different gravel unit unconformably overlies (with angularity) the lower conglomerate ~7 m above the backpack in Panel B (not seen in that photograph). It has 20% yellowish and reddish, very fine sandstone to siltstone clasts that were derived from the Los Vallos Formation (Yeso Group). Note how the gravel is more angular than that seen in the lower conglomerate. This supports the interpretation that the lower conglomerate largely reflects reworking of the Baca Formation, and later, in the late Miocene, uplift along the LSPMFZ resulted in erosion that cut canyons through the San Andres Formation limestone and into the Yeso Group. View to the north.

lenticular beds of conglomerate interbedded with much-finer beds mostly composed of silt to very fine– to fine-grained sand. The gravel is angular to subangular and comprised of mostly pebbles with 7–10% cobbles and 1% boulders. Two clast counts (Fig. 10, Appendix 3) and field observations indicate that the gravel is composed of limestone with 1–5% sandstone that is locally arkosic or micaceous. In contrast to lower strata, there are notable proportions (5–10%) of angular-subangular, reddish-brown to brown chert that resembles authigenic chert in the Bar B and Gray Mesa formations. This gravel correlates with Petrosome D.

Age control

South of the study area (UTM coordinates 324,537 m E, 3,729,294 m N, NAD83, zone 13), a pumiceous sandstone bed was mapped in the transitional zone between the piedmont facies and axial facies of the Sierra Ladrones Formation at an elevation of 4760 ft and between the east and central strands of the Little San Pascual Mountain fault zone (Fig. 1; Koning et al., 2020). The sanidine grains in the sand were analyzed using the $^{40}Ar/^{39}Ar$ technique, as described in the Methods section, and results are summarized in Table 1 and Figure 12. Details of the analyses are in Appendix 1. Two of the 18 dates yield the preferred weighted mean age of 1.641±0.004 Ma (1σ). This age is slightly older (by 30 ky) than a recent, high-precision $^{40}Ar/^{39}Ar$ age of 1.612±0.002 Ma (M. Zimmerer, pers. commun., 2021) but overlaps the lower-precision, published $^{40}Ar/^{39}Ar$ age of 1.635±0.022 Ma for the Otowi Member of the Lower Bandelier Tuff (Spell et al., 1996). With only two grains yielding the preferred weighted mean age, the accuracy of the age is likely not fully represented by the precision of the result; in other words, the full distribution of dates that would provide the most robust mean age is not sampled with n = 2 analysis. Thus, it is likely the two grains sampled in this study are derived from the Lower Bandelier Tuff despite the small age offset. We feel it is defensible to extrapolate the approximate stratigraphic position of this pumiceous bed 5 km northeastward, parallel to the LSPMFZ, into the study area, particularly since no major faults are crossed (i.e., remain in the same fault block), and the

TABLE 1. Summary of $^{40}Ar/^{39}Ar$ analytical data for SM-596-200319. See Appendix 4 for details of full analyses.

Sample	L#	Irradiation	mineral	analysis	N	MSWD	K/Ca±1σ	Age (Ma)±1σ
SM-596-200319	68397	NM-316C	sanidine	mean	2	1.2	40.9±9.8	1.641±0.004

Notes:
1. Isotopic ratios corrected for blank, radioactive decay, and mass discrimination; not corrected for interfering reactions.
2. Errors quoted for individual analyses include analytical error only, without interfering reaction or J uncertainties.
3. Age is weighted mean age. Mean age error is weighted error of the mean, multiplied by the root of the MSWD where MSWD>1, and also incorporates uncertainty in J factors and irradiation correction uncertainties.
4. Isotopic abundances after Steiger and Jäger (1977).
5. Ages calculated relative to FC-2 Fish Canyon Tuff sanidine interlaboratory standard at 28.201 Ma (Kuiper, 2008).
6. Decay Constant (LambdaK (total)) = 5.463e-10/a

Sierra Ladrones Formation is minimally deformed (maximum displacement is only 15 m along a given fault, and strata are subhorizontal). Where found near Popotosa outcrops west of the east strand of the Little San Pascual Mountain fault zone, the elevation of the Sierra Ladrones Formation ranges from 4660 to 4900 ft, so this sample projects to roughly the middle part of the Sierra Ladrones Formation here. A minimum age of 818 ka for the Sierra Ladrones Formation can be inferred because only 12 km southwest of the study area there is an 818.3±10.6 ka basalt flow capping the Sierra Ladrones Formation (Sion et al., 2020; Koning et al., 2020), with no evidence of this basalt subsequently buried by the Santa Fe Group. This results in an interpretation of a 0.8–2.0 Ma age for the Sierra Ladrones Formation in the study area.

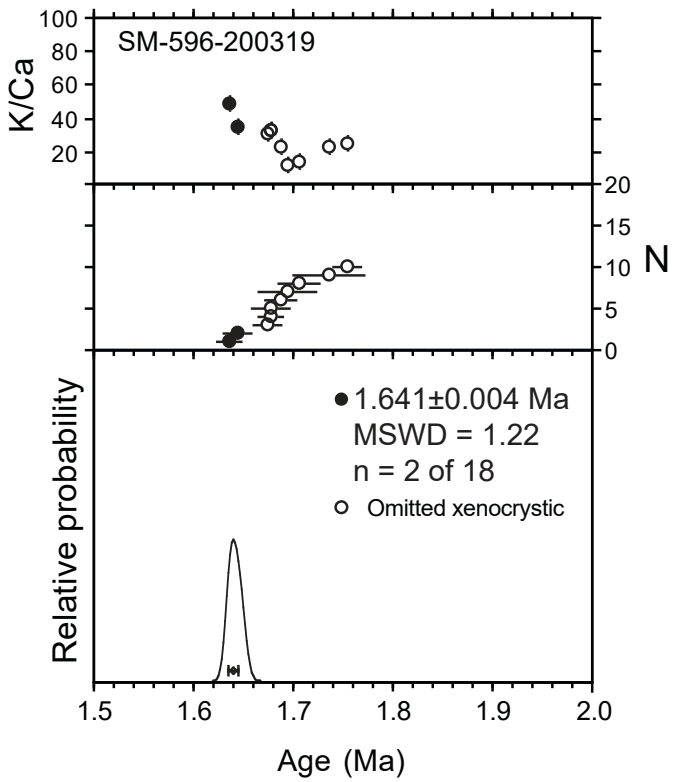

FIGURE 12. Ideograms of detrital sanidine sample from a pumiceous sandstone of the Sierra Ladrones Formation (SM-596-200319). Sample collected at the following UTM coordinates: 324,537 m E, 3,729,294 m N (NAD83, zone 13). Further information on the $^{40}Ar/^{39}Ar$ analyses presented in Appendix 4. Age interpretation courtesy of Matt Heizler.

DISCUSSION

Paleogeographic Evolution

Using the petrosomes and interpreted depositional environments, reasonable paleogeographic interpretations for the period of deposition of the Santa Fe Group can be made. Age control for this interpretation is based on the 0.8–2.0 Ma Sierra Ladrones Formation and correlation of the distinctive, thickly cross-stratified eolian facies in the medial sandstone unit at San Pascualito Butte (Figs. 2, 7). The age control within the Popotosa Formation relies on two possible correlations of this eolian facies to studied Popotosa Formation strata 6–10 km to the northwest (Cikoski, 2010; Chamberlin and Cikoski, 2010). The first correlates the medial sandstone eolian facies to similar facies found in units Tpa and Tpe of Cikoski (2010), which are 12–9 Ma (see Previous Work section). A second possible correlation is between the reddish-brown, relatively fine-grained strata in the upper part of the medial sandstone (units 4–7 of Fig. 7) and the eastern part of unit Tsp of Cikoski (2010). Unit Tsp has not been dated but is younger than the 12–9 Ma eolian facies and younger than an 8.57±0.26 Ma basalt flow (Cikoski, 2010). A field visit to the eastern part of Tsp indicated local fine-grained, basin-floor deposits (muds, silts, very fine– to fine-grained sands) several meters thick; this particular stratigraphic interval of basin floor facies may have extended to the study area described in this paper and perhaps correlates to the upper medial sandstone unit or the basin-floor facies in the intertonguing sandstone-conglomerate unit (e.g., Fig. 8, units 8–10). Using the first correlation (i.e., to units Tpa and Tpe), which we prefer, the medial sandstone unit is interpreted to be 12.0–8.5 Ma. It follows that the underlying lower conglomerate unit is likely middle Miocene (16–12 Ma), and the overlying intertonguing sandstone–conglomerate and the upper conglomerate postdate ca. 10 Ma (preferred age of 10–8 Ma). If the second correlation is correct, then the medial sandstone and younger Popotosa units are 8.5–5.0 Ma. We prefer the first correlation (i.e., to Tpa and Tpe of Cikoski, 2010) because the thickly cross-stratified, eolian deposits are unique in the Popotosa section.

Comparison of the Popotosa Formation petrosomes to those of the Baca and Sierra Ladrones formations is key to our paleogeographic interpretations. The Petrosome A conglomerate of the Baca Formation and the Petrosome D conglomerate of the Sierra Ladrones Formation serve as useful reference sam-

ples of gravel that came from two known paleogeographic settings: pre-volcanic, Laramide deposits (Baca Formation), and the northern part of the western face of the modern-day LSPM (source of gravel found in the piedmont facies of the 2.0–0.8 Ma Sierra Ladrones Formation, assuming the present-day escarpment approximately resembled that at 2.0–0.8 Ma). Another assumption used in the paleogeographic interpretation is the probability of residual Laramide highlands, and that the broad anticline recognized in LSPM (Geddes, 1963a, b) probably was manifested at the start of rifting by a low arch capped by resistant limestone strata.

Gravel in the lower part of the Popotosa Formation, namely the lower conglomerate and the lower unit of the intertonguing sandstone–conglomerate units, are assigned to Petrosome A and resemble the Petrosome A gravels of the Baca Formation. The only appreciable difference in the clast types is the 0–3% presence of Glorieta Sandstone clasts in the Popotosa Formation, which increases up-section (Fig. 10, Appendix 3). Furthermore, the limestone gravels in both are notably subrounded to rounded like those seen in the Baca Formation. Therefore, we interpret that middle Miocene Santa Fe Group deposits in the study area initially reflected reworking of the Baca Formation into a subsiding rift basin (Fig. 13a). Low hills cored by the San Andres Formation limestones were being exhumed, presumably due to footwall uplift. As this exhumation proceeded, more of the lowest San Andres Formation and Glorieta Sandstone was being exposed, and that accounts for the increasing proportion of Glorieta-like clasts up-section in the Petrosome A units (Fig. 10). Although the San Andres Formation has minor chert, this unit contains appreciably less chert than the upper Bar B and Gray Mesa formations (Fig. 4). This observation may explain the conspicuous absence of subangular-angular chert in the lower conglomerate and higher units of the Popotosa Formation.

In the middle Miocene, two alluvial fan systems associated with Petrosome A are inferred to have spilled around either side of the low Laramide arch, probably capped by San Andres Formation limestone, which coincided with the northern, higher part of the LSPM (broad anticline of Geddes, 1963a, b; Fig. 12a). The fans were sourced primarily in the Baca Formation, which varied geographically in its content of Permian clasts. The southern Petrosome A fan lacked reddish-brown Permian clasts and was associated with a drainage that spilled around the south end of the higher part of the LSPM. The Baca Formation here had only minor Permian reddish-brown clasts, as reflected by gravel composition in the southern Baca Formation exposures (see above). The Petrosome A exposures of the lower conglomerate (Tplc) found in Coontail canyon were associated with this southern fan.

The northern fan is represented by the Petrosome A exposures at and north of Fox canyon, and this fan coalesced northward with alluvial fans draining volcanic highlands. Paleoflow here was westerly to southwesterly (Figs. 2, 7). Consistent with the northern Baca Formation exposure at Andesite canyon (Fig. 2, site BF), which has 20–35% reddish-brown, Permian-derived clasts, the northern Petrosome A alluvial fan contained a high amount of Permian-derived clasts potentially derived from eroding Baca Formation in the near-vicinity. The minor presence of greenish to olive-colored sandstones (0–4%) in the inferred northern fan may reflect erosion of Crevasse Canyon Formation sandstone from somewhere east of LSPM. The very sparse granite found in the northern Petrosome A likely was reworked from the Baca Formation, which contains variable granitic clasts (Cather, 2009). In the vicinity of the study area, conglomerates of the Abo Formation are intra-formational (Koning et al., 2020; Lucas et al., this volume; Nelson et al., 2012), and the Bursum Formation lacks conglomerate where it outcrops alongside the LSPM (Koning et al., 2020, 2021), so granite in the northern part of Petrosome A likely did not come from erosion of these Permian strata.

Alluvial fans shrank and the basin floor widened during deposition of the medial sandstone (Fig. 13b), which based on the preferred correlation of this unit to the Tpa and Tpe units of Cikoski (2010) is likely 12–8 Ma. The up-section transition from the lower conglomerate to this sandstone reflects a fining-upward trend and mimics the fining-upward trend seen in ~15 to ~12 Ma strata in the study area of Cikoski (2010). The reason for this basin floor expansion may be due to unspecified paleoclimatic factors or perhaps is attributable to a period of increased slip rates on the east strand of the LSPMFZ. Increased slip rates would presumably have increased accommodation space in the proximal hanging walls of the LSPMFZ, inhibiting the westward progradation of the eastern alluvial fans and keeping their toes closer to the east strand of the LSPMFZ (Fig. 12).

The presence of volcanic gravel in Petrosome A strata overlying the medial sandstone is noteworthy. We infer that the northern fan coalesced northward with another alluvial fan or piedmont that drained a highland underlain by intermediate-composition volcanic rocks to explain the increased percentage of intermediate volcanic clasts in that direction (Fig. 13b). This volcanic-rich alluvial fan is very likely the same fan that deposited unit Tpa in the southeastern part of the study area of Cikoski (2010).

Petrosome B corresponds with the upper unit of the intertonguing sandstone-conglomerate (Fig. 6). Deposition of Petrosome B may have started ca. 10 Ma and perhaps lasted 1 my, based on the absence of paleosols in the unit. Clast imbrication data indicate a westerly paleoflow (ranging from WSW to WNW) for this unit (Fig. 8). There is a clear up-section trend in the composition of the fan gravel in this unit (Fig. 10), in which the proportion of reddish, Permian-derived clasts increases at the expense of limestone clasts, the proportion of yellowish, siltstone–very fine sandstone clasts (probably from the Los Vallos Formation; Fig. 4) increases, and the proportion of Glorieta Sandstone decreases and then disappears. We interpret these observations to indicate that the conglomerate tongues in the Fox Canyon stratigraphic section (Fig. 8) were deposited by a westward-sloping alluvial fan at the mouth of a drainage in the northern part of the western escarpment of LSPM. This drainage was actively incising into these mountains during the deposition of the upper unit of the intertonguing sandstone-conglomerate (Tpsc2), resulting in the progressive removal of the Glorieta Sandstone and lower San Andres

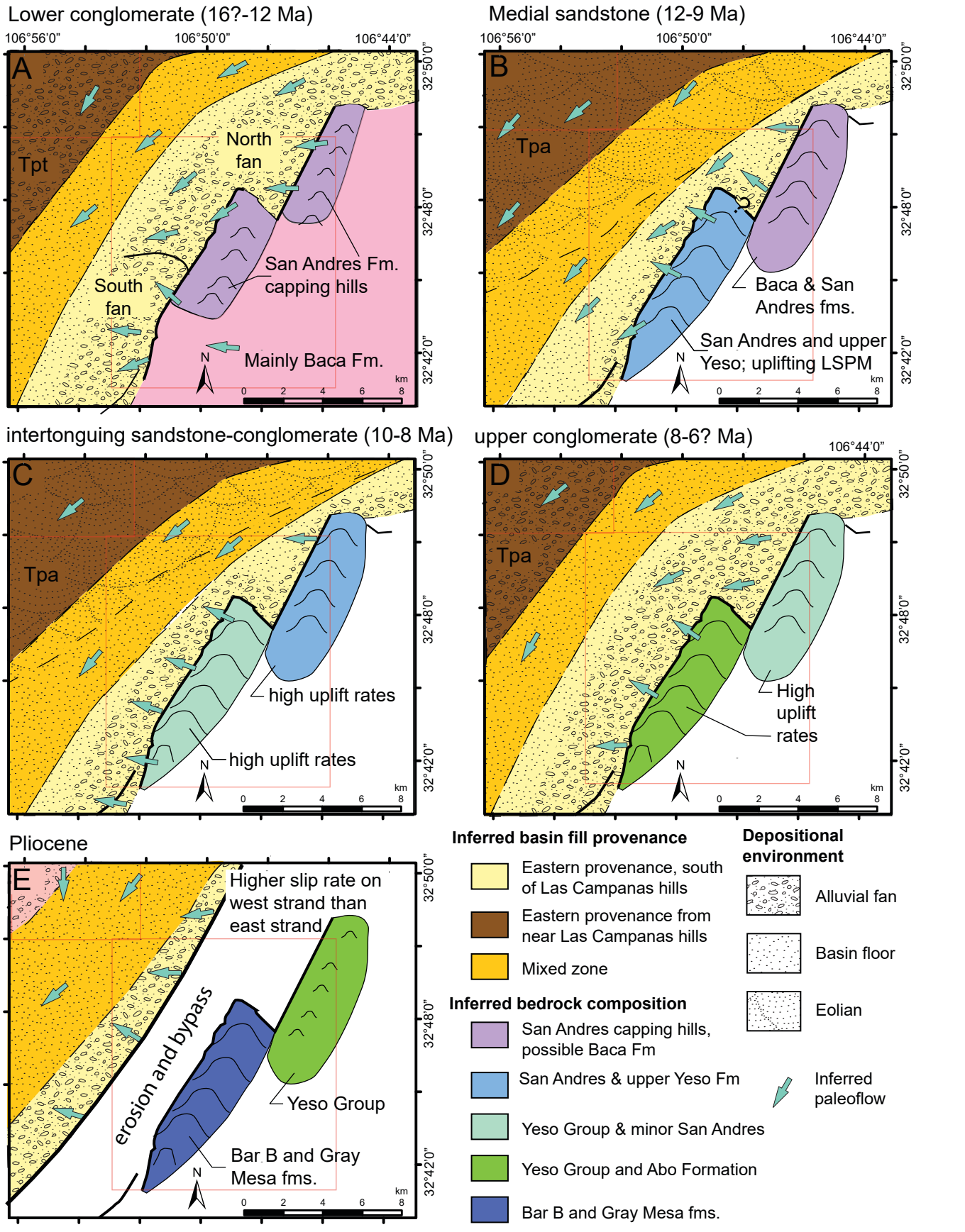

FIGURE 13. Late Miocene paleogeographic maps. Each panel is labeled by the corresponding map unit, except for the Pliocene (lower left). Red boxes are study area boundaries coinciding with those shown on Figure 1. Age ranges are approximate and based on preferred correlation of the medial sandstone stratigraphic unit in this study with units Tpa and Tpe of Cikoski (2010).

Formation and increasing outcrop exposure of the Los Vallos and Meseta Blanca formations. Presumably, this incision was in response to active uplift of the range at this time (Fig. 13c).

The northern Petrosome A fan still existed to the north during deposition of the upper unit of the intertonguing sandstone-conglomerate, because stringers of Petrosome A gravel from that fan can be found in the higher sandstone tongues of the Fox Canyon stratigraphic section (e.g., FC-8d and FC-9, Appendix 2, Fig. 8). The sparseness of these gravels and the fact they are only found within the thick sandstone tongues in the upper sandstone-conglomerate unit suggest that the basin floor facies at this time (e.g., sandstone tongues of units 1a, 4, 8–10, Fig. 8) extended eastward past the northwestern tip of what is now the LSPM and interfingered northeastward with the Petrosome A fan (Fig. 13c). Hard-linkage of the Chert Hill fault with the east strand of the LSPMFZ is possible, and a hypothesized north-south fault northeast of the LSPM (Fig. 13, dotted fault in Fig. 2) could be responsible for this paleodepositional scenario. Such an integrated fault is necessary to create the accommodation space for the youngest Popotosa Formation unit, the upper conglomerate.

Petrosome C, corresponding to the upper conglomerate map unit, is clearly locally derived. Site SFRH (Figs. 2, 3d) exhibits debris flow facies and has 1–3% boulders. To the northeast, clasts are smaller but angular (North-fork Red House stratigraphic section in Figs. 2, 9, Appendix 2). A proximal source area is indicated by the existence of alternating, relatively monolithic beds dominated by: (1) yellowish siltstones–very fine sandstones and yellow-tan, dolomite-rich gravel derived from the Los Vallos Formation, and (2) reddish, very fine– to fine-grained sandstone clasts that match those seen in the Meseta Blanca and Abo formations. The Chert Hill fault and an inferred north-south striking fault to the northeast had to be active at this time to create the accommodation space for this unit (Fig. 13d). The high proportion of reddish, Permian-derived clasts at site SFRH (75%) indicates that most of the northern part of the western face of the LSPM was underlain by Yeso Group and Abo Formation strata. The western extent of the conglomeratic fans (Fig. 13d) and the age of this unit are poorly constrained.

Tectonic Implications

Based on our preferred correlation of the medial sandstone with units Tpe and Tpa in the study area of Cikoski (2010), it would follow that uplift of the LSPM mainly occurred after 12 Ma. Earlier uplift cannot be ruled out; this early uplift may have facilitated removal of relatively thin, late Eocene–early Oligocene volcanic-volcaniclastic strata (see descriptions in Koning et al., 2020, 2021).

The paleogeographic interpretation for the middle Miocene (Fig. 13a) depicts two large alluvial fans (Petrosome A) spilling around hills cored by San Andres Formation limestone. The composition of Baca Formation gravels adjoining the LSPM is consistent with late Eocene paleogeography consisting of highlands underlain by San Andres Formation limestones and variable amounts (increasing to the north) of Yeso Group outcrops. Consequently, there is no reason to invoke post–Baca Formation (post 43–38 Ma—based on minimum age of Baca Formation [Lucas and Williamson, 1993] and maximum depositional ages for the Spears Group of ~43 Ma [Cather et al., in press]), late Eocene through Oligocene removal of the Artesia Group, Triassic strata, and Cretaceous strata in the study area. Therefore, major exhumation appears to have begun in the early–middle Miocene with erosion of the thin(?) Spears Group (this detritus is not observed in the Popotosa Formation in the study area), followed in the middle Miocene by erosion of the Baca Formation and limited contributions from San Andres Formation limestone. This exhumation is likely due to vertical movement along the east strand of the LSPMFZ.

Vertical displacement along the linked east strand of the LSPMFZ and Chert Hill fault (the latter likely linked to a now-buried, north-striking, west-down fault; Fig. 2) would account for the unroofing trend in the Petrosome B gravel seen in the upper intertonguing sandstone-conglomerate unit (Fig. 13c), in which Glorieta-derived clasts disappear up-section and Yeso clasts (yellowish-reddish siltstones, very fine– to fine-grained sandstones, and yellow-tan-brown dolomites) become more abundant.

Relatively high displacement rates of the LSPMFZ continued after deposition of the upper conglomerate (in the late Miocene, perhaps starting at ~8 Ma) through the Quaternary. This resulted in continued uplift and exhumation of the Permian–Pennsylvanian section. Prior to deposition of the 2.0–0.8 Ma Sierra Ladrones Formation in my study area, the entire Permian section and the Bar B Formation were removed from the northern part of the western escarpment of the LSPM. The top of the chert-rich Gray Mesa Formation (Fig. 4) likely attained similar elevations as observed today by 2.0–0.8 Ma, which allowed angular-subangular chert (5–10% of gravel) of Petrosome D to be eroded from this formation and into the piedmont facies of the Sierra Ladrones Formation. The top of the Gray Mesa Formation is about 150 m (500 ft) above the preserved ~1 Ma surface of the Sierra Ladrones Formation, and the amount of missing (removed) strata between the chert-rich Gray Mesa Formation (underlying the highest part of the mountain crest) and the base of the Meseta Blanca Formation is 170 m (ca. 660 ft), based on Figure 4. So, a rough estimate of uplift between ca. 7 Ma (middle of the 8–6 Ma inferred end of Popotosa Formation deposition in my study area) and 2.0–0.8 Ma (deposition age of the preserved Sierra Ladrones Formation on this quadrangle) is 320 m over ca. 6–5 my, or 53–64 m/my. Total exhumation of strata between the middle Miocene and early Pleistocene is ~275 m (stratigraphic interval between the Whiskey Canyon Member, Gray Mesa Formation, and the San Andres Formation).

The angular unconformity on top of the Popotosa Formation is of noteworthy tectonic significance, as it reflects a period of time in which erosion occurred after strata was tilted by as much as 30°. The eastward tilting north of the inferred scissors fault was likely associated with subsidence along the east strand of the LSPMFZ, the Chert Hill fault, and the proposed north-south fault northeast of the present-day LSPM. Thus, activity along this fault trio continued well after deposition of

the upper conglomerate, perhaps until the end of the Miocene. However, the west strand of LSPMFZ became increasingly active as time progressed, probably in the Pliocene, and that activity allowed erosional beveling to occur prior to deposition of the 2.0–0.8 Ma Sierra Ladrones Formation in the study area.

The 15 m of vertical displacement of lower to middle, ca. 2.0–1.0 Ma Sierra Ladrones strata by the east strand of the LSPMFZ (Fig. 3a) gives a throw rate of 7.5–15.0 m/my. This low rate is suggestive of decreased Quaternary slip rates on the east strand of the LSPMFZ compared to the late Miocene–Pliocene, but determination of slip rates on the west strand of the LSPMFZ are needed to make a comprehensive assessment for the entire LSPMFZ.

CONCLUSIONS

Based on detailed mapping of the Popotosa Formation and careful examination of the composition and texture of its gravels, we interpret the following depositional scenario controlled by local activity on rift-related normal faults. Earliest preserved deposits, likely middle Miocene, reflect sedimentation by two large fans that spilled into the basin on either side of the higher part of the LSPM; the LSPM at this time is envisioned as consisting of a low arch cored by the San Andres Formation limestone, a relict from Laramide tectonism. The limestone in this arch was relatively resistant and contributed relatively little detritus during this early stage of Popotosa deposition. Widening of the basin floor, as evident by the widespread deposition of the medial sandstone map unit, may have been controlled by increased displacement rates along the east strand of the LSPM. Fault slip rates were higher in the late Miocene after ca. 10 Ma, leading to unroofing of the northern LSPM. During 12–8 Ma, the east strand of the LSPMFZ linked with a now-buried, north-striking and west-down fault northeast of the LSPM via the Chert Hill fault, which allowed subsidence north of the LSPM and accumulation of the upper conglomerate. Following erosion of the Mesozoic section in the Laramide, about 275 m of exhumation occurred between the middle Miocene and early Quaternary. Assuming the LSPM were relatively low in elevation when easily erodible Permian strata were exposed in the middle of the late Miocene (ca. 7 Ma), an uplift rate of 53–64 m/my is calculated for the LSPMFZ between 7 Ma and 1 Ma. In the Pliocene, increasing throw rates occurred on the west strand of the LSPMFZ relative to the east strand, causing the erosional beveling of tilted strata in the block between the east and west strands of the LSPMFZ prior to onlap of the Sierra Ladrones Formation.

ACKNOWLEDGMENTS

We are grateful to Scott Elrick and W. John Nelson for drafting up the bedrock stratigraphic column of Figure 4. Dan also appreciates the help of his daughters, Claire and Adele, in measuring the Fox Canyon stratigraphic section. Reviews by Steven Cather, Shari Kelley, and Ryan Leary improved the manuscript.

REFERENCES

Allmendinger, R.W., Cardozo, N., and Fisher, D.M., 2012, Structural Geology Algorithms: Vectors and Tensors: Cambridge, Cambridge University Press, 302 p.

Cardozo, N., and Allmendinger, R.W., 2013, Spherical projections with OSXStereonet: Computers & Geosciences, v. 51, p. 193–205.

Cather, S.M., 2009, Stratigraphy and structure of the Laramide Carthage-La Joya Basin, central New Mexico: New Mexico Geological Society, Guidebook 25, p. 227–234.

Cather, S.M., Heizler, M.T., and McIntosh, W.C., in press, Middle Eocene to Pliocene Volcanic, Volcaniclastic, and Intrusive Rocks of the Quebradas Region, *in* Cather, S.M., and Koning, D.J., eds., Geology of the Quebradas Region, Socorro County, Central New Mexico: New Mexico Bureau of Geology and Mineral Resources Memoir 51.

Chamberlin, R.M., and Cikoski, C.T., 2010, Geologic map of the Indian Well Wilderness quadrangle, Socorro County, New Mexico: New Mexico Bureau of Geology and Mineral Resources, Open-file Geologic Map 201, scale 1:24,000.

Cikoski, C., 2010, Geology of Neogene basin fill of the Indian Well Wilderness 7.5' quadrangle, central Rio Grande rift, New Mexico [M.S. thesis]: Socorro, New Mexico Institute of Mining and Technology, 160 p.

Geddes, R.W., 1963a, Structural geology of Little San Pasqual Mountain and the adjacent Rio Grande trough [M.S. thesis]: Socorro, New Mexico Institute of Mining and Technology, 64 p.

Geddes, R.W., 1963b, Geology of Little San Pasqual Mountain: New Mexico Geological Society, Guidebook 14, p. 197–203.

Heizler, M.T., Karlstrom, K.E., Albonico, M., Hereford, R., Beard, S., Cather, S., Crossey, L., and Sundell, K., 2021, Detrital sanidine $^{40}Ar/^{39}Ar$ dating confirms <2 Ma age of Crooked Ridge paleoriver and deep denudation of the southwestern Colorado Plateau: Geosphere, v. 17, p. 438–454, https://doi.org/10.1130/GES02319.1.

Jochems, A.P., and Love, D.W., compilers, 2016, Fault number 1995, Little San Pasqual fault, *in* Quaternary fault and fold database of the United States: U.S. Geological Survey website, https://earthquakes.usgs.gov/hazards/qfaults (accessed 04/14/2022).

Koning, D.J., Pearthree, K.S., Jochems, A.P., and Love, D.W., 2020, Geologic map of the San Marcial 7.5-minute quadrangle, Socorro County, New Mexico: New Mexico Bureau of Geology and Mineral Resources, Open-File Map 284, 1 sheet, scale 1:24,000.

Koning, D.J., Nelson, W.J., Elrick, S., and Attia, S., 2021, Geologic map of the Little San Pascual Mountain 7.5-minute quadrangle, Socorro County, New Mexico: New Mexico Bureau of Geology and Mineral Resources, Open-File Map 296, scale 1:24,000.

Kuiper, K.F., Deino, A., Hilgen, F.J., Krijgsman, W., Renne, P.R., and Wijbrans, J.R., 2008, Synchronizing the rock clocks of Earth history: Science, v. 320, p. 500–504, https://doi.org/10.1126.science.1154339.

Lucas, S.G., and Williamson, T.E., 1993, Eocene vertebrates and late Laramide stratigraphy of New Mexico: New Mexico Museum of Natural History and Science, Bulletin 2, p. 145–158.

Lucas, S.G., Krainer, K., Allen, B.D., and Barrick, J.E., 2017, The Pennsylvanian section in the Little San Pascual Mountain, Socorro County, New Mexico: New Mexico Museum of Natural History and Science, Bulletin 77, p. 287–307.

Lucas, S.G., Krainer, K., and Nelson, W.J., this volume, Permian stratigraphy east of Socorro, central New Mexico: New Mexico Geological Society, Guidebook 72.

Morgan, G.S., Lander, E.B., Cikoski, C., Chamberlin, R.M., Love, D.W., and Peters, L., 2009, The oreodont Merychyus major major (Mammalia: Artiodactyla: Oreodontidae) from the Miocene Popotosa Formation, Bosque del Apache National Wildlife Refuge, Socorro County, central New Mexico: New Mexico Geology, v. 31, p. 91–103.

Nelson, W.J., Lucas, S.G., Krainer, K., McLemore, V.T., and Elrick, S., 2012, Geology of the Fra Cristobal Mountains, New Mexico: New Mexico Geological Society, Guidebook 63, p. 195–210.

Sion, B.D., Phillips, F.M., Axen, G.J., Harrison, B.J., Love, D.W., and Zimmerer, M.J., 2020, Chronology of terraces in the Rio Grande rift, Socorro Basin, New Mexico: Implications for terrace formation: Geosphere, v. 16, p. 1–23, https//doi.org/10.1130/GES02220.1.

Seiger, R.H., and Jäger, E., 1977, Subcommission on geochronology: Convention on the use of decay constants in geo- and cosmochronology: Earth and Planetary Science Letters, v. 36, issue 3, p. 359–362.

Spell, T.L., McDougall, I., and Doulgeris, A.P., 1996, Cerro Toledo Rhyolite, Jemez volcanic field, New Mexico: $^{40}Ar/^{39}Ar$ geochronology of eruptions between two caldera-forming events: Geological Society of America Bulletin, v. 108, no. 12, p. 1549–1566.

Wentworth, 1922, A scale of grade and clast terms for clastic sediments: Journal of Geology, v. 30, no. 5, p. 377–392.

Appendices can be found at https://nmgs.nmt.edu/repository/index.cfml?rid=2022001